Interaction of radiation with free convection in an open cavity

C. Balaji and S. P. Venkateshan
Heat Transfer and Thermal Power Laboratory, Department of Mechanical Engineering, Indian Institute of Technology, Madras, India

This paper reports the numerical results of the fundamental problem of interaction of surface radiation with free convection in an open cavity with air as the intervening medium. Rayleigh numbers (based on height) in the laminar range 10^4–10^8 have been considered in the present study. Surface radiation was found to alter the basic flow pattern as well as the overall thermal performance substantially. A physical insight into the effect of radiation has been provided and correlations have been developed for convective as well as radiative transfer based on the numerical results.

Keywords: natural convection; radiation enhancement; correlations; vorticity; stream function

Introduction

The importance of natural convection as a mode of heat dissipation without any expenditure of high-grade energy need not be overemphasized. The present study addresses three basic points.

First, instead of a closed cavity, an open cavity with a continuous intake of fresh air and exhaust of heated air is far more advantageous with no attendant problems like stratification, which occurs in a completely closed cavity. Hence, it offers one method of heat dissipation from electronic equipment and, to protect the component from external disturbances, housing the component in a slot (open cavity) may be required, although mounting it on a vertical flat plate will be advantageous for both convective and radiative heat transfer. The effect of radiation on convection in a closed cavity has been considered by Balaji and Venkateshan (1993).

Second, the present study may simulate the cooling of a microcomponent placed in a slot similar to the one considered by Behnia and de Vahl Davis (1990). However, in the present study the whole left wall is considered an isothermal heat source. This condition may be realized if there is a large number of small, flush-mounted, heat-generating components placed along the left wall. The same geometry has been considered by Lage et al. (1992) but with a different application in mind (i.e., ash hopper design of power plants). In the case of Behnia and de Vahl Davis, the cavity spacing is on the order of a few tens of millimeters and the effect of radiation has not been considered. In the case of Lage et al., the cavity spacing is on the order of a few hundreds of millimeters and a simplistic model has been used for radiation. Lage et al. have worked out the convective heat flux independent of radiation by assuming various temperatures on the right wall (Figure 1). By using these convective fluxes, the radiosity equations have been solved to determine the equilibrium temperature of the right and bottom wall, which together have been assumed to be at one temperature. A realistic model would involve the assumption that both the right and bottom walls attain temperatures that are determined by a balance between convection and radiation. This means that the flow equations cannot be solved independently of the radiation equations and hence the two must be solved simultaneously. Notwithstanding the fact that this procedure is computationally more involved, it is indeed necessary from the viewpoint of consistency in specifying boundary conditions on the walls, but also from the viewpoint of proper appreciation of the physics associated with the problem. This point will be clearly brought out in the section on results and discussion.

Third, the present study presents comprehensive correlations for determining the overall heat transfer for a wide range of

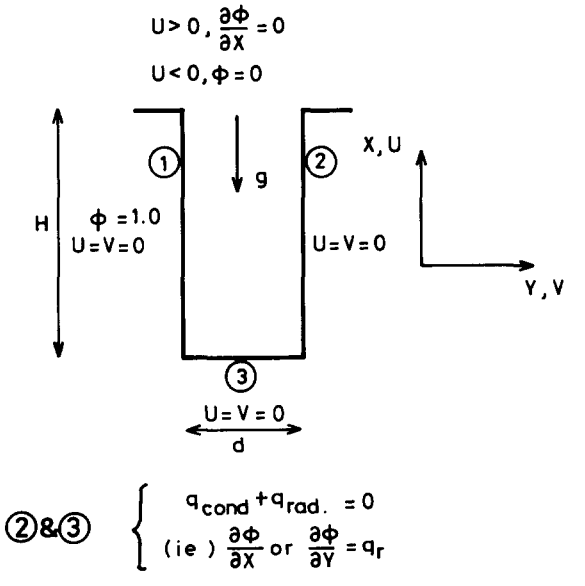

Figure 1 Problem geometry

Address reprint requests to Professor Venkateshan at the Heat Transfer and Thermal Power Laboratory, Department of Mechanical Engineering, Indian Institute of Technology, Madras, 600 036, India.

Received 10 January 1994; accepted 28 March 1994

parameters and also discusses the limitations in realizing the thermal boundary conditions used.

Mathematical formulation

The flow and heat transfer in the two-dimensional cavity are governed by the conservation of mass, momentum and energy. The schematic of the cavity with a height of H, spacing of d along with the system of coordinates is given in Figure 1. The governing equations in the normalized form, in the vorticity-stream function formulation are

$$U\frac{\partial\omega}{\partial X}+V\frac{\partial\omega}{\partial Y}=\mathrm{Pr}\,[\nabla^2\omega]-\mathrm{Ra}\frac{\partial\phi}{\partial Y} \tag{1}$$

$$\nabla^2\psi=-\mathrm{Pr}\,\omega \tag{2}$$

$$\nabla^2\phi=U\frac{\partial\phi}{\partial X}+V\frac{\partial\phi}{\partial Y} \tag{3}$$

The fluid under consideration is air (Pr = 0.71).

Boundary conditions on solid walls

Free convection problem.

Bottom wall:

$X = 0,\ 0 < Y < 2,\ \psi = \text{constant},$

$$\omega=-\frac{1}{\mathrm{Pr}}\frac{\partial^2\psi}{\partial X^2},\ \frac{\partial\phi}{\partial X}=0 \tag{4}$$

Left wall:

$Y = 0,\ 0 < X < 2AR,\ \psi = \text{constant},$

$$\omega=-\frac{1}{\mathrm{Pr}}\frac{\partial^2\psi}{\partial Y^2},\ \phi=1.0 \tag{5}$$

Right wall:

$Y = 2,\ 0 < X < 2AR,\ \psi = \text{constant},$

$$\omega=-\frac{1}{\mathrm{Pr}}\frac{\partial^2\psi}{\partial Y^2},\ \frac{\partial\phi}{\partial Y}=0 \tag{6}$$

Free convection with surface radiation. The boundary conditions for vorticity and stream function are the same as those specified earlier. However, the thermal boundary conditions on the bottom and right walls are based on a balance between radiation and convection (i.e., the walls are truly adiabatic).

Bottom wall:

$$X=0,\ 0<Y<2,\ \frac{\partial\phi}{\partial X}=N_{RC}(j-i) \tag{7}$$

Right wall:

$$Y=0,\ 0<X<2AR,\ \frac{\partial\phi}{\partial Y}=N_{RC}(j-i) \tag{8}$$

Notation

$a_1 \ldots, g_1$	Constants in the expression for stream function, Equation 9
AR	Aspect ratio, H/d
d	Spacing, m
E_R	Enhancement due to radiation, $\frac{q_{\text{overall (with radiation)}}}{q_{\text{overall (without radiation)}}}$, Equation 20
g	Acceleration due to gravity, m/s^2
Gr_d	Grashof number based on d, $gB(T_1 - T_2)d^3/\nu^2$
Gr_H	Grashof number based on H, $gB(T_1 - T_2)H^3/\nu^2$
H	Height of the cavity, m
i	Elemental dimensionless irradiation, $I/\sigma T_1^4$
I	Elemental irradiation, W/m^2
j	Elemental dimensionless radiosity, $J/\sigma T_1^4$
J	Elemental radiosity, W/m^2
k	Thermal conductivity of fluid, W/mK
N_{RC}	Radiation conduction interaction parameter, $\sigma T_1^4 d/[(T_1 - T_2)k]$
Nu_c	Convection Nusselt number, $-(\partial\phi/\partial Y)_{Y=0 \text{ or } 2}$ or $-(\partial\phi/\partial X)_{X=0}$
Nu_C	(based on H) $\mathrm{Nu}_C AR$
$\overline{\mathrm{Nu}}_c$	Mean convection Nusselt number, $\int_0^2 \frac{(\mathrm{Nu}_c)}{2}dY$ or $\int_0^{2AR}\frac{(\mathrm{Nu}_c)}{2AR}dX$
$\overline{\mathrm{Nu}}_o$	Overall Nusselt number, $\overline{\mathrm{Nu}}_c + \overline{\mathrm{Nu}}_R$
Nu_R	Radiation Nusselt number, $N_{RC}(j - i)$
Nu_R	(based on H) $\mathrm{Nu}_R AR$
$\overline{\mathrm{Nu}}_R$	Mean radiation Nusselt number, $\int_0^2 \frac{(\mathrm{Nu}_R)}{2}dY$ or $\int_0^{2AR}\frac{(\mathrm{Nu}_R)}{2AR}dX$
Pr	Prandtl number, ν/α
q_R	Elemental radiative heat flux, $(J - I)$ W/m^2
Ra_d	Rayleigh number based on d, Gr_d Pr
Ra_H	Rayleigh number based on H, Gr_H Pr
T	Temperature, K
T_1	Temperature of the left wall of the enclosure, K
T_2	Temperature of the ambient, K
T_R	Temperature ratio, T_2/T_1
u	Vertical velocity, m/s
U	Dimensionless vertical velocity, ud/α
v	Horizontal or cross velocity, m/s
V	Dimensionless horizontal velocity, vd/α
x	Vertical coordinate, m
X	Dimensionless vertical coordinate, x/d
y	Horizontal coordinate, m
Y	Dimensionless horizontal coordinate, y/d

Greek Symbols

α	Thermal diffusivity of the fluid, m^2/s
β	Cubical expansion coefficient of fluid, 1/K
ε	Emissivity of the three walls
ν	Kinematic viscosity of the fluid, m^2/s
ϕ	Dimensionless temperature, $(T - T_2)/(T_1 - T_2)$
ψ'	Stream function, m^2/s
ψ	Dimensionless stream function, ψ'/α
σ	Stefan Boltzmann constant, 5.67×10^{-8} W/m^{2}K^4
ω'	Vorticity, $1/S$
ω	Dimensionless vorticity, $\omega' d^2/\nu$

Boundary conditions on the top

Energy conditions. When the vertical velocity U is negative (i.e., flow is into the cavity), the temperature T is T_2 (i.e., $\phi = 0$), that of the ambient. When the vertical velocity U is positive, then the required condition is $\partial\phi/\partial X = 0$. This condition is quite easy to justify. By the time the fluid exits the cavity, it has already picked up all the heat it can and hence the derivative of the temperature at the top is essentially zero.

Momentum conditions. For the momentum conditions, different options have been suggested. One option is to assume V (cross velocity) to be zero and the other condition is X derivative of vertical velocity $\partial U/\partial X$ is zero. From a physical standpoint, cross velocity to be zero is justifiable. The derivative of the vertical velocity being zero means that the fluid velocity profile is invariant with respect to X. It resembles the fully developed flow condition. This condition has been used by Lage et al. (1992). The other condition that has been used is $\partial V/\partial X = 0$ (Chan and Tien 1985). This is more a smoothing condition, as it means that the second derivative of stream function $\partial^2\psi/\partial X^2$ is zero.

Both the conditions that have been used highlight certain important points. For a tall cavity, at the top it is only the vertical velocity and its gradients (along the Y direction) that are important. The horizontal velocity and its derivative are negligibly small. Experimental confirmation that these boundary conditions are adequate to study the heat transfer and flow characteristics of the cavity has been reported in Chan and Tien (1985). It can be demonstrated that both conditions are actually very similar and, in terms of physical interpretation, lead to the same conclusions.

Let the stream function near the top boundary be represented by a cubic polynomial in X and Y (Figure 2). The cubic polynomial was chosen so that the second derivative of ψ can still be a function of X and Y, which is less restrictive than a second-degree polynomial that results in both $\partial^2\psi/\partial X^2$ and $\partial^2\psi/\partial Y^2$ being constants.

$$\psi = a_1 + b_1X + c_1X^2 + d_1X^3 + e_1Y + f_1Y^2 + g_1Y^3 \tag{9}$$

There are seven constants and seven conditions required: ψ_1, ψ_2, ψ_3 are known; ω_2 (at the solid wall) and ω_3 (at the interior node) are also known. Two additional conditions are

$$V = 0 \tag{10}$$

$$\frac{\partial V}{\partial X} = 0 \quad \text{or} \quad \frac{\partial U}{\partial X} = 0 \tag{11}$$

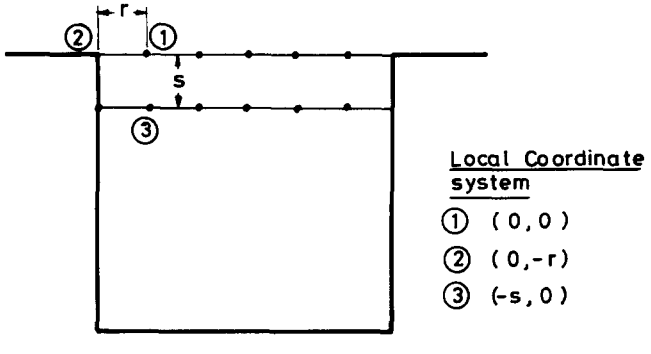

Figure 2 Local coordinate system for generation of vorticity and stream-function conditions

Application of the five known conditions with Equations 10 and 11 gives

$$\omega_1 = \omega_3 + \frac{(\psi_3 - \psi_1)}{S^2} \tag{12}$$

where

$$S = (X_3 - X_1)$$

But to satisfy the compatibility criterion that $V = 0$, ψ_3 must equal ψ_1. Hence, $\omega_1 = \omega_3$. So, the boundary condition on vorticity turns out to be $\partial\omega/\partial X = 0$. Thus vorticity is invariant with respect to X on the top boundary. It can now be proved that this actually means that the condition $\partial U/\partial X = 0$, used by Lage et al. (1992), will be automatically satisfied.

$$\omega = \frac{\partial V}{\partial X} - \frac{\partial U}{\partial Y} \tag{13}$$

and when

$$\frac{\partial V}{\partial X} = 0$$

$$\omega \sim \frac{\partial U}{\partial Y} \tag{14}$$

The condition that has been derived for vorticity implies that $\omega \neq f(X)$ at the top. Hence, ω can be a constant or a function of Y,

$$f(Y) \approx \frac{\partial U}{\partial Y}$$

$$U \sim g(Y) \tag{15}$$

which means $\partial U/\partial X = 0$ at the top. This is indeed the condition used by Lage et al. In terms of physical interpretation, it means that a cross placed in the fluid will experience the same rotation at the top and at a station near the top but just below it. In fact, it means that the velocity can be deemed to be fully developed and that the U profile is invariant with X. So it can be seen that two related but yet different boundary conditions in the primitive variable method lead to the same result in the $\omega - \psi$ method, and ψ and ω can indeed be specified on a free boundary. It will be shown later that with these specifications convergent solutions are obtained to the governing equations.

Method of solution

Free convection equations

Equations 1, 2 and 3 in nondimensional form were solved by a finite-volume method based on Gosman et al. (1969) with a 31 × 31 nonuniform grid system. Nonuniform grids with very fine grids near the walls were generated with a cosine function and were used for the horizontal direction (Y). Closely spaced grids were also used near the bottom walls for the vertical direction (X). The grid pattern used is shown in Figure 3. Underrelaxation with a relaxation parameter of 0.5 was used for all three equations to obtain convergent results. Upwinding was used for the inertia terms to ensure that the convection coefficients that arise in the algorithm are positive or at the worst zero, but never negative, thus ensuring stable and convergent solutions. The maximum error in temperature at $Ra_d = 10^6$ was 0.2 percent on temperature. The local Nusselt numbers were evaluated using three-point interpolation formulae and the mean Nusselt number was determined using the extended trapezoidal rule for nonuniform step sizes.

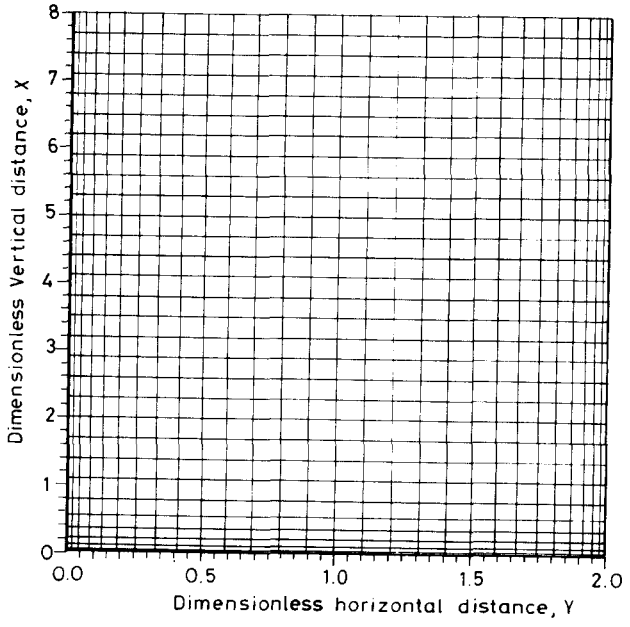

Figure 3 Grid pattern of the cavity

Radiation equations

The grids used for convection were retained for radiation. Radiative transfer from the walls was evaluated based on the enclosure method, with each wall being divided into 30 zones. The view factors were evaluated using Hottel's crossed-string method. The appropriate radiosity equations in nondimensional form are

$$j_i = \varepsilon_i(T_i/T_1)^4 + (1 - \varepsilon_i) \sum_{j=1}^{120} F_{ij} j_j,\ i = 1 - 120 \tag{16}$$

The first term on the right-hand side represents the emission term and the second term is the reflected radiation. The summation is over all the irradiation terms for that particular wall element. The radiosities are updated in every iteration for the flow equations, because they are dependent on the temperature of the wall elements. After all the radiosities are known, the irradiations are evaluated and net radiant flux from each zone is evaluated. This is balanced against conduction through the boundary condition equation.

$$\frac{\partial \phi}{\partial X} = N_{RC}(j - i)$$

or

$$\frac{\partial \phi}{\partial Y} = N_{RC}(j - i) \tag{17}$$

depending on the respective element on the bottom or right wall, as the case may be. The new value of nondimensional temperature is determined on the bottom and right walls. This updated value of temperature is used to solve the flow equations in the ensuing iteration and the procedure is repeated until convergence is achieved.

Calculation of overall heat transfer from the cavity

The overall heat transfer from the cavity is made up of two parts—the convective part and the radiative part. Since the right wall and bottom wall are truly adiabatic, the sum of the convective heat transfer from the two walls will be exactly equal to the sum of the radiative heat fluxes received by them, but with an opposite sign. Hence, the overall heat flux for the cavity based on the base area is given by

$$q_{\text{total}} = q_{\text{conv(left)}} + q_{\text{rad(left)}} \tag{18}$$

where the radiation heat transfer from the left wall is given by

$$q_{\text{rad(left)}} = q_{\text{rad(right)}} + q_{\text{rad(bottom)}} + q_{\text{rad(top)}} \tag{19}$$

As stated earlier, ignoring the sign, $q_{\text{conv(right)}} = q_{\text{rad(right)}}$ and $q_{\text{conv(bottom)}} = q_{\text{rad(bottom)}}$. Hence, the enhancement factor E_R due to radiation defined as the ratio of overall heat transfer when radiation is present ($\varepsilon \neq 0$) to the overall heat transfer when radiation is not there ($\varepsilon = 0$) is given by

$$E_R = \frac{q_{\text{conv(left)}} + q_{\text{rad(left)}}}{q_{\text{conv(left)}}} \tag{20}$$

Since the flow is predominantly a boundary-layer type, the coupled boundary condition for the bottom wall does not greatly affect the convective heat transfer from the left wall itself. Stated more explicitly, $q_{\text{conv(left)}}$ remains the same with and without radiation in the limits of numerical accuracy.

Results and discussion

Validation for pure natural convection ($\varepsilon = 0$)

For the case of pure natural convection, the code developed in the present study is validated with that of Lage et al. (1992). For purposes of validation, the right wall is assumed to be at the same temperature as that of the left wall (i.e., nondimensional temperature $\phi = 1.0$) and the bottom wall is insulated, which represents one of the cases considered by Lage et al. for pure natural convection. Results were obtained for aspect ratios 2–5 and Rayleigh numbers (Ra_d) from 10^5–10^7. However, the results were correlated with the Rayleigh number based on H to facilitate comparison with Lage et al. The Nusselt numbers, which by definition in the present study mean Nusselt number based on spacing d, were modified so that they are based on H. Also the Rayleigh numbers were modified to be based on H in order to facilitiate comparison with Lage et al. Nu_H was correlated in the form of $\text{Nu}_H = a(\text{Ra}_H)^b$ and a and b were determined to be 0.436 and 0.259, respectively. In all other places in the present text, both the Rayleigh number and the Nusselt number are based on spacing d unless otherwise stated. The agreement between the data and correlation seen in Figure 4 is very good. The values of a and b reported in Lage et al. are 0.42–0.44 and 0.26, respectively. The excellent agreement between the two results is a strong indication of the soundness of the present code. Besides, it also vindicates the specification of the vorticity and stream-function conditions at the free boundary used in the present solution procedure.

For a related geometry, but with the opening on the right side (Figure 5), Chan and Tien (1985) have given numerical as well as experimental results. They found that the outgoing flow for $\text{Ra}_d = 10^6$ is around 30 percent, with the experiment and numerical calculations differing by 2 percent. These results are of primary interest because the comparison of these trends with the present results will validate the present results even further.

In this study, to facilitate comparison with the data of Chan and Tien, the governing equations were modified and one test run was performed to achieve strict validation against their carefully done experiments. The source term in the X momentum and Y momentum equations become $\text{Ra}\ \phi\ \text{Cos}\ \theta$ and $\text{Ra}\ \phi\ \text{Sin}\ \theta$, respectively, where θ is the tilt angle of the cavity with the vertical. Hence, the source term in the

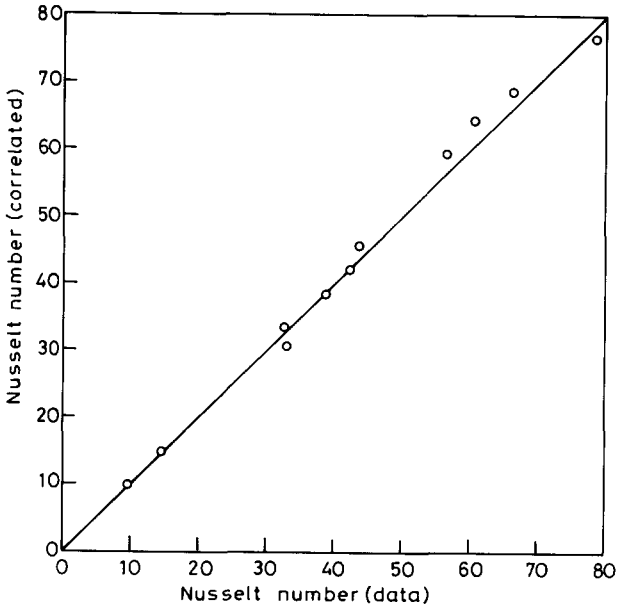

Figure 4 Comparison of the Nusselt number data and correlation for the pure convection problem

vorticity equation becomes

$$-\mathrm{Ra}\left[\mathrm{Cos}\,\theta\,\frac{\partial\phi}{\partial Y}-\mathrm{Sin}\,\theta\,\frac{\partial\phi}{\partial X}\right] \tag{21}$$

When θ is zero, the cavity becomes a vertical cavity and the source term is $-\mathrm{Ra}\,\partial\phi/\partial Y$. When $\theta = 90°$, the source term is $\mathrm{Ra}\,\partial\phi/\partial X$ and the cavity now becomes the one considered by Chan and Tien. With this modification in the governing equations, along with the necessary modifications in the boundary conditions as given in Figure 5, results were obtained for $\mathrm{Ra}_d = 10^6$ and the aspect ratio ($AR = 7$) similar to the one considered in their study. The mean Nusselt number was determined to be 14.4, as opposed to 15 obtained by Chan and Tien. The error is around 4 percent and the agreement is very good. The temperature and velocity profiles are in excellent agreement (qualitatively) and the outgoing flow was found to occupy about 32 percent of the opening area, which is very close to the value of 30 percent obtained by them.

The present numerical investigation has thus been validated against a standard numerical as well as a standard experimental result. It speaks for the efficiency of the quick, but all the same, accurate finite-volume method with the voriticity-stream function formulation. More importantly, it also proves that the boundary conditions that have been derived for vorticity and stream function are adequate to study the flow and heat transfer characteristics of the problem under consideration.

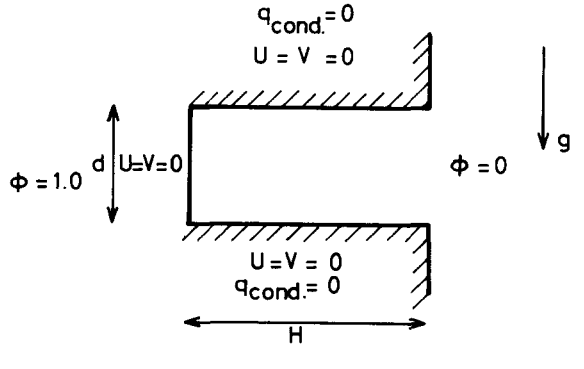

Figure 5 Problem geometry of Chan and Tien (1985)

Validation for radiation: the case of $\varepsilon = 1$

In order to validate the radiation routine, a typical case of all the three walls being at the same temperature (T_1) was considered. The convection routines were suppressed to study the effect of radiation alone. The radiation Nusselt number based on spacing d for a temperature ratio of 0.8 and $N_{RC} = 10$ was determined to be 5.89. Because the three walls are isothermal and the enclosure is black, one expects the heat transfer from the top to be equal to the heat transfer from the base (if there were not sidewalls), given by $N_{RC}[1 - T_R^4]$, which in this case equals 5.904. Indeed, the agreement between the simple calculation and the one obtained by the elaborate zone analysis is excellent and the error is only around 0.2 percent. However, for the actual problem being considered (Figure 1), there is a strong interaction between convection and radiation as the right and bottom walls float at a temperature governed by convective and radiative balance. Hence, a zone analysis with 120 zones indeed becomes necessary to ensure grid compatibility between radiation and convection. This is a prerequisite for stable and convergent solutions.

Effect of radiation

In this section, attention is focused on the influence of radiation and hence the extreme cases of $\varepsilon = 0$ and $\varepsilon = 1$ will alone be discussed. However, the correlations to be presented in the following section include emissivities in the range 0–1. Figure 6 shows the vertical velocity profile at the top of the cavity for $\mathrm{Ra}_d = 500{,}000$ and aspect ratio = 4 when ε of all the walls is 0 (i.e., there is no radiation). It can be seen that the outgoing flow area is around 18 percent of the total area. The figure also clearly indicates sharpness of the velocity profile toward the heated left wall and confirms the boundary-layer type of flow. Figure 7 highlights the velocity profile for the same Ra_d and aspect ratio, but with the ε of all the walls being 1. If one takes a closer look at Figures 6 and 7, it can be seen that instead of one flow loop occurring in the pure convection case, there are

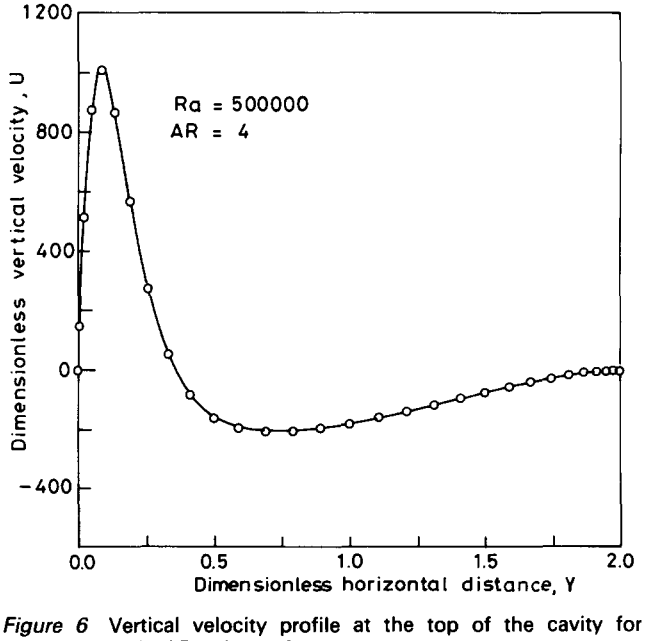

Figure 6 Vertical velocity profile at the top of the cavity for $\mathrm{Ra}_d = 500{,}000$; $AR = 4$; $\varepsilon = 0$

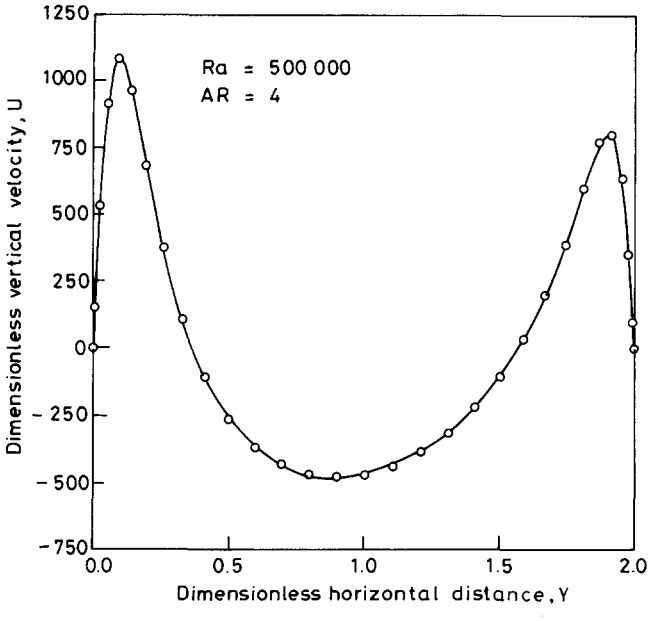

Figure 7 Vertical velocity profile at the top for $Ra_d = 500{,}000$; $AR = 4$; $\varepsilon = 1$

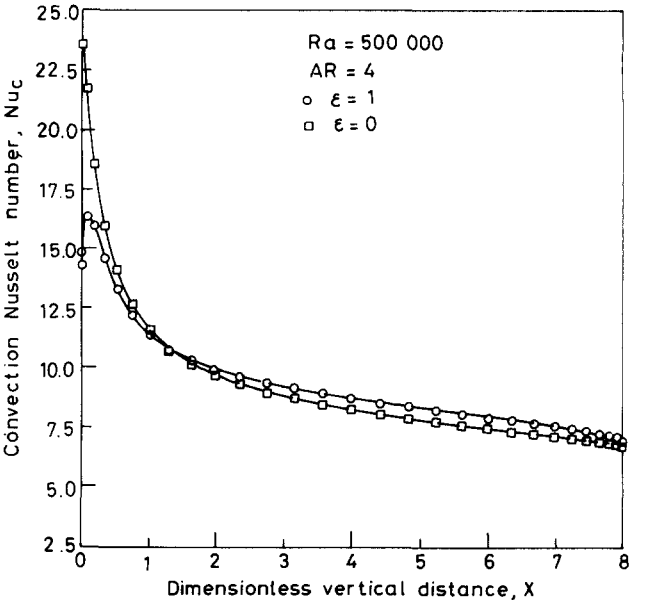

Figure 9 Nusselt number distribution along the left wall for $Ra_d = 500{,}000$; $Ar = 4$; $\varepsilon = 0$; $\varepsilon = 1$

two loops when radiation is present. So the radiative heat transfer from the left wall has heated both the right and the bottom walls, and, under equilibrium, these two walls lose heat convectively to the air. Thus, radiation changes the basic flow physics associated with the problem completely. Bear in mind that the fluid under consideration (air) is nonparticipating and all of the effects mentioned earlier are purely due to wall radiation. Hence, the interaction between radiation and free convection in this class of problem is indeed very strong and disproves the common claim that at low temperature levels radiation can be ignored. Figure 8 shows the temperature distribution across the cavity for the same set of parameters ($Ra_d = 500{,}000$; $AR = 4$; $\varepsilon = 1$) for all the walls. It can be seen that the bottom wall is substantially heated because of radiation. If one calculates the mean temperature for this case ($T_1 = 100°C$, $T_2 = 25°C$), it would be 55°C. If there is no radiation, the same wall would have been at an average temperature close to 33°C. The convection Nusselt number distribution along the left wall for the two cases is given in Figure 9. Though there is a slight change in the nature of the distribution near the bottom, the mean Nusselt number from the left wall is almost constant for both cases. Figure 10 gives the distribution of temperature along the right wall for the same parameters. The average temperature of the wall turns out to be around 62.5°C. The enhancement due to radiation (E_R) for this set of parameters is around 1.8, which means radiation heat transfer is 80 percent of the convective heat transfer. Figure 11 shows the Nusselt number distribution along the right wall.

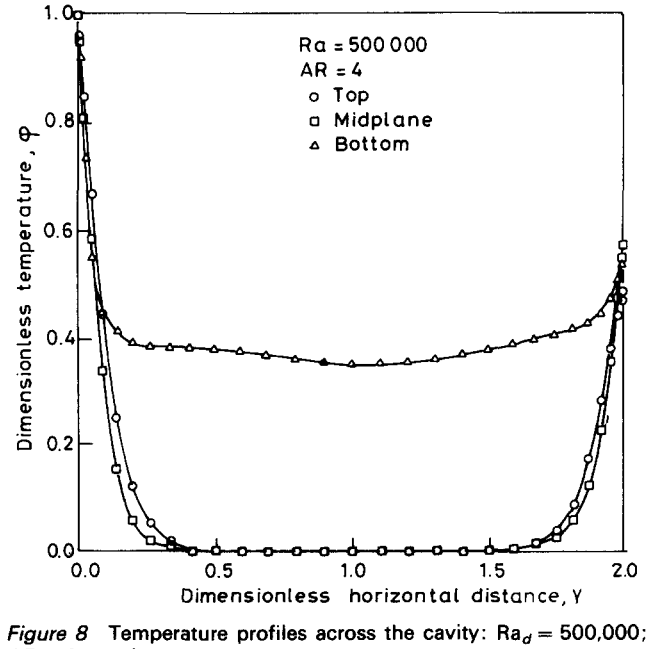

Figure 8 Temperature profiles across the cavity: $Ra_d = 500{,}000$; $AR = 4$; $\varepsilon = 1$

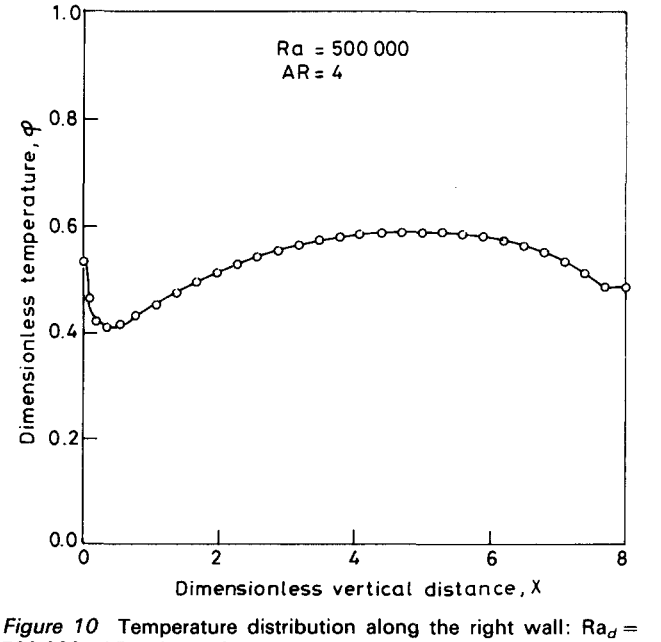

Figure 10 Temperature distribution along the right wall: $Ra_d = 500{,}000$; $AR = 4$; $\varepsilon = 1$

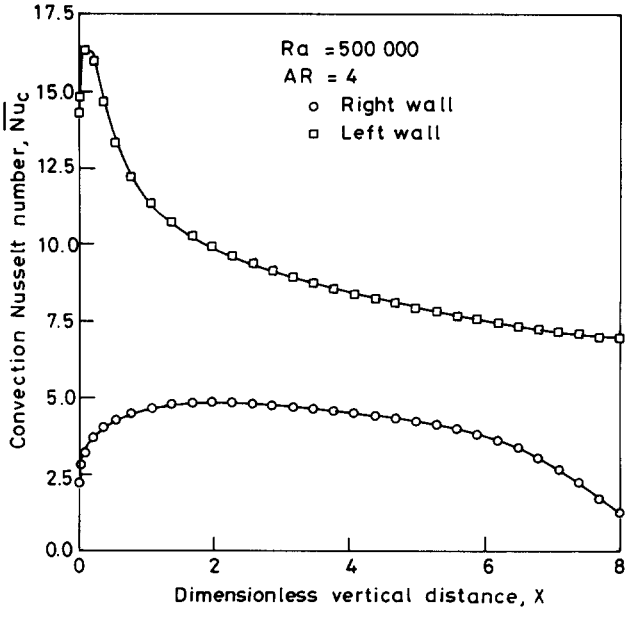

Figure 11 Nusselt number distribution along the left and right wall: $Ra_d = 500{,}000$; $AR = 4$; $\varepsilon = 1$

The rather peculiar nature of distribution is because of the nonisothermal nature of the right wall. The Nusselt number distribution along the left wall has also been included to get an idea about the relative rates of convection from the left and right walls. Figure 12 highlights the variation of the radiation Nusselt number along the left wall for the same set of parameters. It is seen that even though the left wall is isothermal, the radiation Nusselt number has a strong distribution, basically because of the nonisothermality of the other walls.

Correlations

The range of parameters for which calculations have been done are $10^4 \leq Ra_H \leq 10^8$, $0 \leq \varepsilon \leq 1$, $0.75 \leq T_R \leq 0.85$, $9 \leq N_{RC} \leq 30$, and $1 \leq AR \leq 5$. All the walls were assumed to be of the same emissivity. Based on a large set of numerical data (35 data points), the convection Nusselt number ($\overline{Nu}_C$) based on H for convenience, correlates as

$$\overline{Nu}_C \text{ (based on } H) = 0.426\,(Gr_H^{0.254})\,(N_{RC}/(N_{RC+1}))^{1.81}(1+\varepsilon)^{-0.039} \quad (22)$$

The Grashof number exponent of 0.254 is close to the normally quoted values for this geometry (Lage et al. 1992). N_{RC} is chosen in its present form because it is actually a superfluous parameter if only one fluid is considered. But if the temperature level changes, while the temperature difference between the left wall and ambient remain the same, then $\overline{Nu}_C$ can be mildly affected because of radiative effects. For this reason, N_{RC} is retained in the correlation. For instance, if Gr changes by 20 percent then $\overline{Nu}_C$ changes by 4.7 percent, whereas if N_{RC} changes by 20 percent then $\overline{Nu}_C$ changes only by 0.9 percent. Hence, $\overline{Nu}_C$ is a weak function of N_{RC}. The $1+\varepsilon$ term has a small negative exponent, which means that at higher ε, the drop in the convective Nusselt number increases. But even at $\varepsilon = 1$, this drop is only 3 percent. Hence, one can conclude that convection from the left wall is relatively insensitive to radiation. From a physical standpoint, this seems reasonable, as the convective flow is predominantly a boundary-layer flow (unlike a closed cavity) and therefore the right wall does not have any influence on convection from the left. The excellent agreement between the correlation and the data can be seen in Figure 13. Gr has been used for convenience, as usually results reported for air use Gr in preference to Ra.

Correlation for radiation:

$$\overline{Nu}_R \text{ (based in } H) = 1.306\,Gr_H^{-0.079}(1 - T_R^4)^{1.223}\,N_{RC}^{1.21}\,\varepsilon^{0.875}A \quad (23)$$

Radiative flux is proportional to $T_1^4 - T_2^4$. Hence, the temperature ratio is correlated in the form given in Equation 23. In regards to T_1^4, it appears in the N_{RC} term. As ε increases $\overline{Nu}_R$ increases and hence the power law form is used for ε. The influence of convection is brought out by the Gr term. At this juncture, it needs to be emphasised that $\overline{Nu}_R$ actually includes the convection from the right and bottom walls, as these two walls are truly adiabatic. Hence, there is an inherent coupling

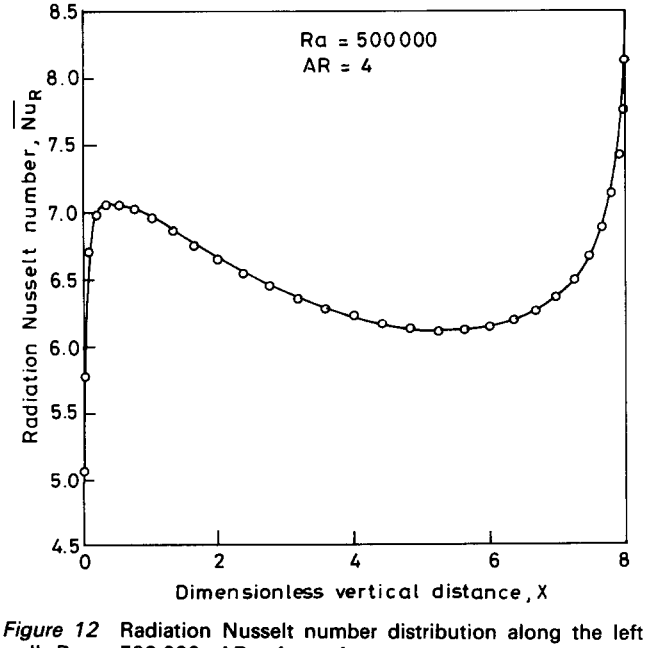

Figure 12 Radiation Nusselt number distribution along the left wall: $Ra_d = 500{,}000$; $AR = 4$; $\varepsilon = 1$

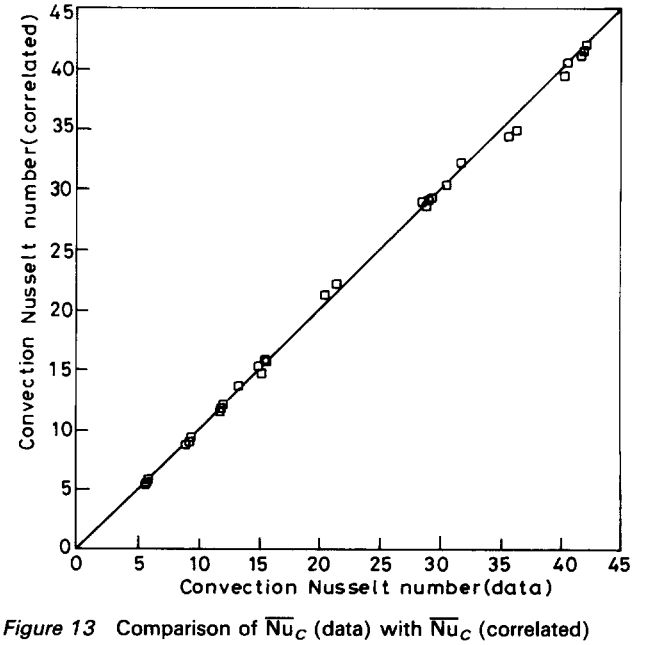

Figure 13 Comparison of $\overline{Nu}_C$ (data) with $\overline{Nu}_C$ (correlated)

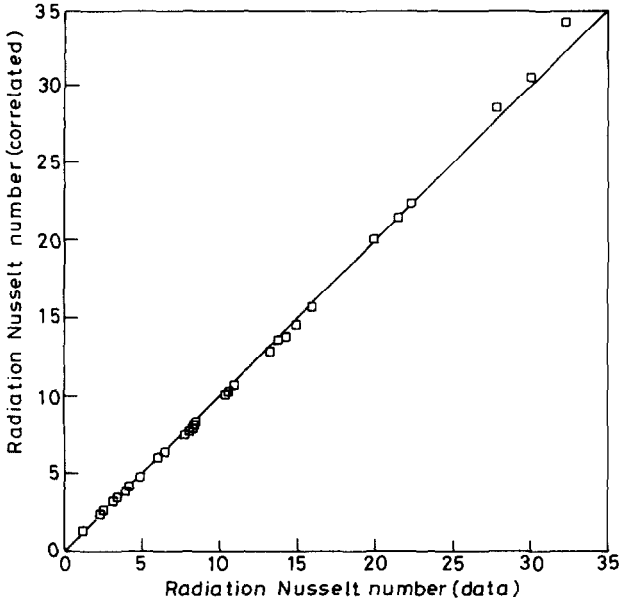

Figure 14 Comparison of $\overline{Nu}_R$ (data) with $\overline{Nu}_R$ (correlated)

in the open cavity problem. The goodness of the fit can be seen in Figure 14.

Effect of conduction

It is instructive to examine the thermal conditions on the walls a little more closely. The adiabatic condition used in the present study for the right and bottom walls can be realized if these walls are sufficiently thick and are made of a material of very low thermal conductivity. Opposed to this is the case of a thin wall composed of material of very high thermal conductivity. Representative calculations were performed for this case, in which the whole cavity will be at one temperature. Typically for $AR = 2$ and $Ra_d = 5.2 \times 10^5$, $T_1 = 100°C$ and $T_2 = 25°C$, and $\varepsilon = 1$, the adiabatic model considered in the present study gave an overall Nusselt number of 20, with a radiation contribution (q_{rad}/q_{conv}) amounting to 85 percent. The perfectly conducting cavity gave an overall Nusselt number of 29.1, with a radiation contribution of 51 percent. Hence, radiation plays a very significant role even in the case of the asymptotic limit of the whole cavity being isothermal.

General comments

The analysis presented in the present paper considers only laminar flow. If Ra_H exceeds 10^9 or so, then the coupled equations of turbulent natural convection and radiation have to be solved simultaneously. Also, the present study assumes that the external environment (air) has no influence on the results. This assumption is valid because of the high value of the vertical velocity at the top end of the cavity, as opposed to the low velocity prevailing in the ambient. However, this assumption may not be valid for cavities with $AR < 1$, which is outside the range of parameters of the present study.

Conclusions

The present study reported the influence of thermal conditions, particularly radiation, on a relatively new geometry—an open cavity. Correlations based on the numerical results were presented for both convection and radiation after a rigorous validation. Radiation was found to enhance overall heat transfer substantially (50–80 percent) depending on the radiative parameters. Lastly, the study has also brought out the efficacy of the vorticity and stream-function method for this class of problems.

References

Balaji, C. and Venkateshan, S. P. 1993. Interaction of surface radiation with free convection in a square cavity. *International Journal of Heat and Fluid Flow*, **14**, 260–267

Behnia, M. and de Vahl Davis, G. 1990. Natural convection cooling of an electronic component in a slot. *Proceedings of the Ninth International Heat Transfer Conference* (Vol. 2) Jerusalem, 343–348

Chan, Y. L. and Tien, C. L. 1985. A numerical study of two-dimensional laminar natural convection in shallow open cavities. *International Journal of Heat and Mass Transfer* **28**, 601–612

Gosman, A. D., Pun, W. M., Runchal, A. K., Spalding, D. B. and Wolfshtein, M. 1969. *Heat and Mass Transfer in Recirculating Flows.* Academic Press, London

Lage, J. L., Lim, J. S. and Bejan, A. 1992. Natural convection with radiation in a cavity with open top end. *Journal of Heat Transfer*, **114**, 479–486